Theor Chem Acc (2002) 107:357–361
DOI 10.1007/s00214-002-0340-3

Theoretical
Chemistry Accounts

Regular article

Linear stability analysis of a reaction–diffusion model of solid-phase combustion

Rui Zhu[1], **Qian Shu Li**[1,2]

[1] School of Chemical Engineering and Material Science, Beijing Institute of Technology, Beijing 100081, China
[2] National key Laboratory of Theoretical and Computational Chemistry, Jilin University, Changchun, Jilin 130023, China

Received: 6 November 2001 / Accepted: 25 March 2002 / Published online: 13 June 2002

Abstract. The dynamic behavior of a reaction–diffusion model of solid-phase combustion is investigated by using the linear stability analysis method. The diffusion coefficients of the oxygen gas and the vapor of the combustible solid (Mg) are taken as two controlling parameters in the analysis. The bifurcation map obtained shows three dynamic regions. Region I only shows stable combustion. Regions II and III both show stable combustion and oscillatory combustion depending on the ratio of the two diffusion coefficients. Interestingly region II also shows a small range of a bistable state consisting of a stable focus and an oscillating state, which is like the critical phenomena in phase transitions. The results indicate that the occurrence of oscillating combustion requires that the value of the diffusion coefficient of the Mg vapor should be comparable to or less than that of the oxygen gas at the same temperature.

Key words: Nonlinear chemistry dynamics – Linear stability analysis – Solid-phase combustion – Dynamic behavior

1 Introduction

Rich nonlinear dynamic phenomena in chemical systems have been observed experimentally and investigated theoretically in the past few decades [1, 2, 3]. As a subfamily of nonlinear chemistry dynamics, nonlinear dynamics in combustion reactions has drawn considerable attention in the past 2 decades. The pioneering work on nonisothermal combustion processes was done by Uppal et al. [4, 5] and Kubicek et al. [6]. The mechanisms for some gas-phase combustion systems have been well examined, among which the most successfully studied one is the H_2–O_2 combustion system [7, 8, 9, 10]. Recently, a more complex nonlinear phenomenon – chemical waves formed in premixed gas combustion – has been investigated [11, 12]. Compared with research on the nonlinear dynamic behavior of gas-phase combustion systems, less work has been done on that of solid-phase combustion systems owing to the complex interactions of chemical and physical processes. The first solid-phase combustion system that showed oscillation was recorded in 1898. Since then, several other solid-phase systems with oscillatory combustion behavior have been reported [13, 14]. In 1978, Matkowsky and Sivashinsky [15] constructed a mathematical model for the system reported in Ref. [14], and found its Hopf bifurcation points by nonlinear analysis of this model. It should be noted that this model merely concerns solid–gas reactions. In 1990, Bayliss and Matkowsky [16] modified their previous model into two models, which are related to solid–gas reactions and liquid–gas reactions, respectively. They took the same controlling parameter as that employed in Ref. [15], which was a product of a dimensionless activation energy and a factor that is a measure of the difference between the nondimensionalized temperature of unburned reactants and the combustion products. They detected Hopf bifurcations again and, moreover, two ways to chaos.

To our knowledge, the models of combustion systems studied previously explored only solid–gas reactions, liquid–gas reactions, or gas–gas reactions. Here, however, we investigate a combustion model in relation to both solid–gas and gas–gas reactions, in which the diffusion of gases – a ubiquitous physical process – is considered. In other words, we investigate a reaction–diffusion model of solid combustion.

This model comes from a recently discovered oscillatory solid-phase combustion system, i.e., a mixture of reducing agent Mg, oxidant NH_4ClO_4, and frequency-modulating species $K_2Cr_2O_7$ [17]. The partial pressures of reacting gases, i.e. oxygen and Mg vapor, as the major dynamic controlling factors in this model were considered in Ref. [17]. On the other hand, diffusion coefficients are

Correspondence to: Q. S. Li
e-mail: qsli@bit.edu.cn

closely related to partial pressures, so they were chosen as the major controlling parameters. It is worth noting that the diffusion coefficients of oxygen and Mg vapor were considered in Ref. [17] to be identical. We think such simplification may not uncover the effect of gas diffusion on the dynamic behavior of this system. Thus, in the present work we select the diffusion coefficients of the two kinds of reacting gases as different controlling parameters, and study how they affect the dynamic behavior of the model system by using the linear stability analysis method.

2 Model and methods

2.1 Model

The model can be written as follows [17],

$$\mathrm{Mg(s)} + \mathrm{O_2} \xrightarrow{k_1} \mathrm{MgO(s)} + a\mathrm{Mg(g)}, \tag{1}$$

$$[b\mathrm{Mg(g)} + \mathrm{Mg(s)}] + \mathrm{O_2} \xrightarrow{k_2} \mathrm{MgO(s)} + c\mathrm{Mg(g)}, \tag{2}$$

$$\mathrm{Mg(g)} + \mathrm{O_{2env}(constant)} \xrightarrow{k_3} \mathrm{MgO(s)}, \tag{3}$$

$$\mathrm{Mg(g)} \xrightarrow{k_\mathrm{M}} \mathrm{Mg(g)_{env}(constant)}, \tag{4}$$

$$\mathrm{O_2} \xleftarrow{k_\mathrm{O}} \mathrm{O_{2env}(constant)}, \tag{5}$$

where Mg(s) represents the solid of Mg, Mg(g) the Mg vapor close to the surface of Mg(s), MgO the solid oxidation product of Mg, and $\mathrm{Mg(g)_{env}}$ and $\mathrm{O_{2env}}$ the Mg(g) and $\mathrm{O_2}$ in the environment. k_1, k_2, and k_3 are reaction constants, and k_M and k_O are diffusion coefficients for Mg(g) and $\mathrm{O_2}$, respectively. a, b, and c are adjustable parameters. Processes 1 and 2 are the solid–gas reactions occurring close to the surface of Mg(s), process 3 is the gas–gas reaction occurring in the environment, and processes 4 and 5 are physical diffusion processes in relation to Mg(g) and $\mathrm{O_2}$, respectively, whose directions of net diffusion are shown by the arrows. Note that the $\mathrm{O_2}$ in processes 1 and 2 is close to the surface of Mg(s), which is provided by diffusion process 5.

For the simplicity of analysis, let X denote $\mathrm{O_2}$, Y denote Mg(g), which reduces processes 1–5 to the following forms only relating to gases,

$$X \xrightarrow{k_1} aY \tag{6}$$

$$X + bY \xrightarrow{k_2} cY \tag{7}$$

$$Y \xrightarrow{k_3} \tag{8}$$

$$Y \xrightarrow{k_\mathrm{M}} \tag{9}$$

$$X \xleftarrow{k_\mathrm{O}} \tag{10}$$

On the basis of the mass-action law, the reaction-rate equations are given by

$$\mathrm{d}X/\mathrm{d}t = -k_1X - k_2XY^b + k_\mathrm{O}(X_0 - X) \tag{11}$$

and

$$\mathrm{d}Y/\mathrm{d}t = ak_1X + (c-b)k_2XY^b - k_3Y + k_\mathrm{M}(Y_0 - Y). \tag{12}$$

For brevity, the following dimensionless equations are introduced for the previous dynamic equations:

$$\mathrm{d}x/\mathrm{d}\tau = -wx - xy^b + (1-x)/t_0 \tag{13}$$

and

$$\mathrm{d}y/\mathrm{d}\tau = awx + (c-b)xy^b - vy + (y_0 - y)/t_1, \tag{14}$$

with the scalings $x = X/X_0$, $y = Y/X_0$, $\tau = k_2X_0^b t$, $w = k_1/k_2X_0^b$, $v = k_3/k_2X_0^b$, $t_0 = k_2X_0^b/k_\mathrm{O}$, and $t_1 = k_2X_0^b/k_\mathrm{M}$.

In order to compare our results with the results of experiments, we use the same numerical parameters as those in Ref. [17], i.e., let $a = 1$, $b = 2$, $c = 3$, $w = 1/650$, $v = 1/20$, and $y_0 = 0.006$. As such, the dynamic equations for a certain system of this type are obtained as

$$\mathrm{d}x/\mathrm{d}\tau = -(1/650)x - xy^2 + (1-x)/t_0 \tag{15}$$

and

$$\mathrm{d}y/\mathrm{d}\tau = (1/650)x + xy^2 - (1/20)y + (0.006 - y)/t_1. \tag{16}$$

After these deductions, t_0 and t_1, respectively relating to the diffusion coefficients of $\mathrm{O_2}$ and Mg(g), become two dynamic controlling parameters in the following analysis.

2.2 Methods

First, the steady-state solutions of Eqs. (15) and (16) are obtained by zeroing them and keeping the real solutions only. Afterwards, the stability of the steady points is obtained by analyzing the eigenvalues of the Jacobian matrix of the Eqs. (15) and (16) at the corresponding steady points. This procedure is referred to as linear stability analysis [18]. As already stated, there are two changeable parameters, t_0 and t_1, in the analysis. For convenience, we let t_0 be fixed, then draw the curve of y^* against t_1, where y^* is the y-coordinate of the steady points gained by zeroing Eqs. (15) and (16). In addition, whether this model has periodic solutions or other complicated solutions can be judged by analyzing the corresponding bifurcation diagram of the system, which is plotted using the Poincaré section method [19]. In the following analysis, keep in mind that stable-state solutions represent stable combustion and that periodic solutions represent oscillatory combustion.

3 Results and discussion

A bifurcation map that plots two curves of critical steady points in t_0–t_1 space is shown in Fig. 1. Figure 1 clearly shows three dynamic regions, and they are described in detail in the following.

Region I ($47.5 > t_0 > 0$): As shown in Fig. 1, there are two critical steady points in region I, but it should be noted that C_l is always on the right of C_u, indicating that

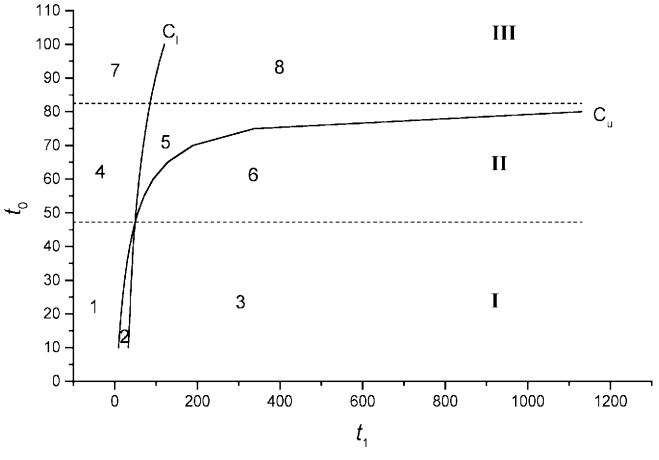

Fig. 1. Bifurcation map in the t_0–t_1 parameter space. Three dynamic regions marked I, II, and III. C_l and C_u denote the lower and upper critical steady points, respectively. Region I is split into three areas by C_l and C_u, marked 1, 2, and 3, which represent monostability, bistability, and monstability, respectively. Region II is split into three areas, areas 4 and 6 being monostable, area 5 in oscillation. Region III is divided into areas 7 and 8, being monostable and in oscillation, respectively

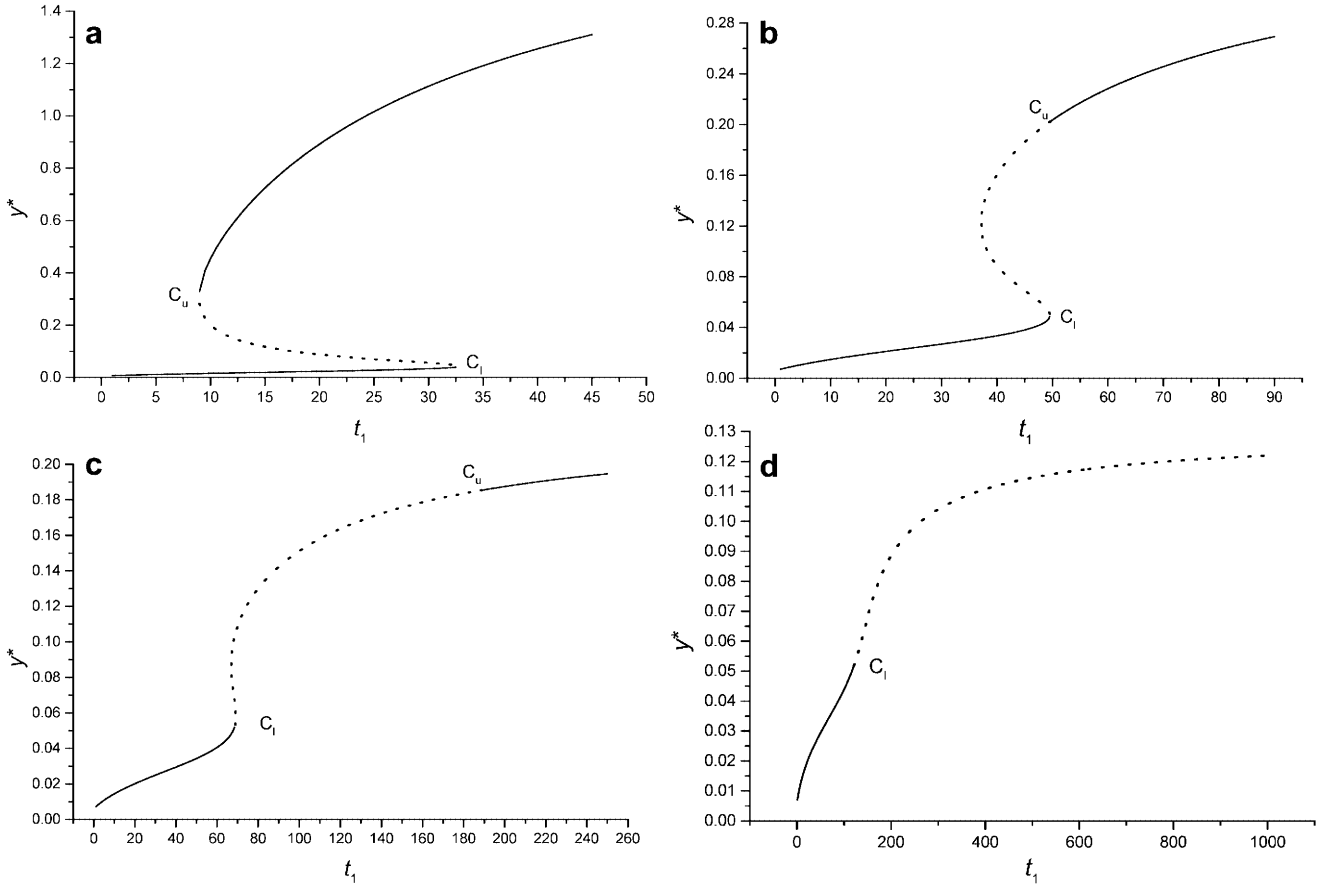

Fig. 2a–d. Steady points diagrams (only variation of y^* versus t_1 is plotted). The *solid curves* denote stable steady points and the *broken curves* denote unstable steady points. **a** $t_0 = 10$, a case in region I. Both the left of C_u and the right of C_l are monostable, but the part between C_u and C_l is bistable. **b** $t_0 = 47.5$. This is the critical case transiting from region I to region II, whose C_u and C_l have the same t_1. It is monostable with a big leap. **c** $t_0 = 70$, a case in region II. C_l and C_u are two Hopf bifurcation points, in which C_l is at $t_1 = 69.13$ (in comparison with the bifurcation point B in Fig. 3) and C_u at $t_1 = 189.19$ **d** $t_0 = 100$, a case in region III. Only a monostable and an oscillating state exist. C_l is the unique Hopf bifurcation point

this region is characterized as bistable. A typical case of such bistability for $t_0 = 10$ is shown in Fig. 2a, where the solid curve represents stable steady points and the dashed curve unstable ones. In this region, no limit cycle emerges, indicating that combustion is stable no matter how t_1 varies. However, the case changes when $t_0 = 47.5$, a critical case corresponding to the crossing in Fig. 1. See Fig. 2b for $t_0 = 47.5$; C_u and C_l have the same t_1. We can see clearly that the bistability has changed to monostability with a big leap. After $t_0 > 47.5$, the system goes into region II, the most interesting region here.

Region II ($82.6 > t_0 > 47.5$): As indicated in Fig. 1, after $t_0 > 47.5$, the relative positions of C_l and C_u in region II are reversed from those in region I, i.e., C_l is on the left of C_u. In this region, we take the case of $t_0 = 70$, for example. See Fig. 2c for $t_0 = 70$, compared with Fig. 2a for $t_0 = 10$, the upper unstable section has walked beyond the lower right stable endpoint, i.e., an intermittence has come into being between the two parts of monostability, suggesting the possibility of observing more interesting dynamic behavior, such as Hopf bifurcation. On the basis of the bifurcation diagram in Fig. 3 for $t_0 = 70$, we indeed detect two bifurcation points, one at $t_1 = 68.00$, the

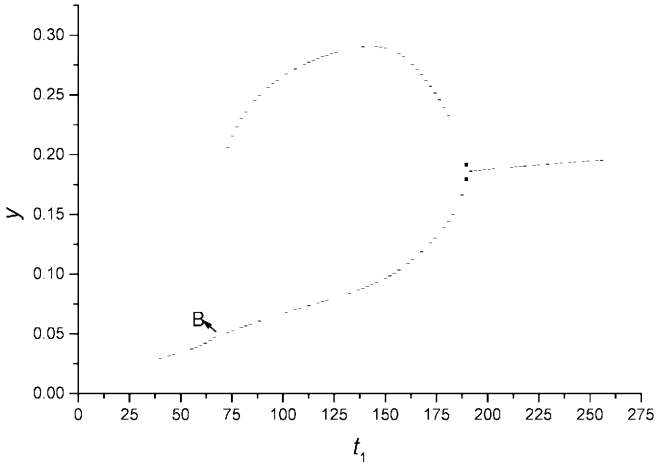

Fig. 3. Bifurcation diagram for $t_0 = 70$. The value of t_1 at the bifurcation point B is 68.00

other at $t_1 = 189.20$. However, what surprises us more is that in Fig. 2c, C_l, the turning point from a stable focus to an unstable focus obtained by linear stability analysis, is at $t_1 = 69.13$, different from $t_1 = 68.00$ ob-

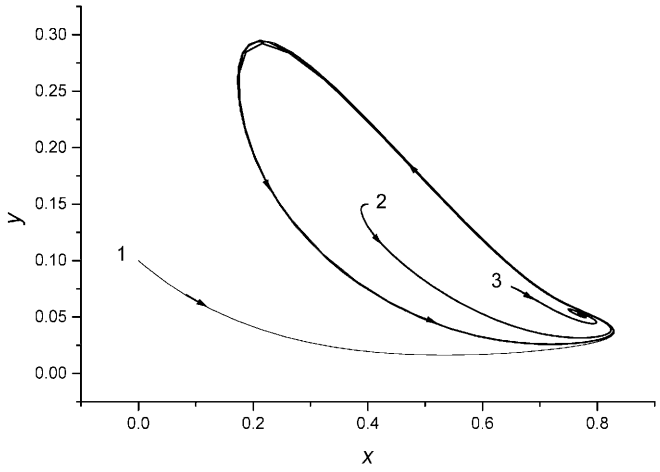

Fig. 4. Illustration of the coexisting state of one stable point and one limit cycle in phase space, modeled at $t_0 = 70.00$ and $t_1 = 69.00$. Points 1, 2, and 3 are three starting points, in which points 1 and 2 spiral inwards and outwards, respectively, – the same limit cycle–, while point 3 spirals inwards – a stable point

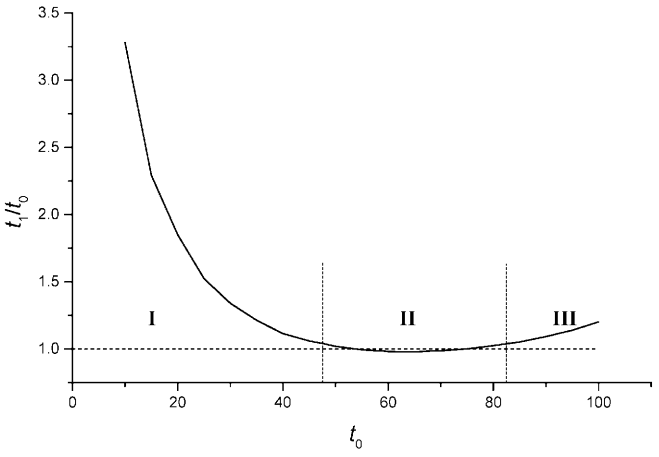

Fig. 5. The curve of variation of t_1/t_0 at C_1 versus t_0. Regions I, II, and III correspond to those in Fig. 1. Note that in region II, the values of t_1/t_0 almost equal unity, while in region III, the values of t_1/t_0 are larger than unity, and increase with the increment of the value of t_0

tained from the bifurcation diagram. In terms of Hopf bifurcation theory, C_1 must be a well-defined Hopf bifurcation point. That is to say, in the case of $t_0 = 70$, there seems to be two attracting basins, respectively corresponding to a stable point and a limit cycle between the range of $t_1 = 68.00$–69.13. This is proved to be right. The results of numerical integration at $t_0 = 70.00$ and $t_1 = 69.00$ are shown in Fig. 4. Points 1 and 2 spiral inwards and outwards, respectively, – the same limit cycle, while point 3 spiral inwards – a stable point. Another point of interest in this coexisting case is that the stable point is very close to the limit cycle in the phase space, indicating that the stable point is "unstable", because once a tiny perturbation is introduced, it would probably walk into the limit cycle. This phenomenon seems like the critical phenomena in phase transitions. For example, although overheated water can exist in reality, it is unstable because if a bit of dust is introduced it will probably vaporize suddenly. The following area ranging from $t_1 = 69.13$ to 189.19 is only characterized as an oscillation. When $t_1 > 189.19$, the limit cycles disappear, and the stable points appear again. Though only the case of $t_0 = 70$ is discussed here, the other cases in region II are the same to $t_0 = 70$. In addition, another hallmark in region II is that the value of t_1/t_0 at C_1 almost equals unity (see Fig. 5).

From Fig. 1, we can see that the upper dashed line at $t_0 = 82.60$ is the asymptote for C_u, beyond which the system will enter region III.

Region III ($t_0 > 82.60$): In region III, there is only one critical steady point, C_1, and it is a Hopf bifurcation point. In contrast to region II, there is not a coexisting state, and the value of t_1/t_0 at C_1 is larger than unity and increases with the increment of t_0. In summary, only two states exist in region III: a monostable state and an oscillating state.

All the results are summarized in Table 1, giving the essential nonlinear dynamic features of the model in different dynamic regions. From Table 1, we can see that only two combustion states exist, i.e., stable combustion and oscillating combustion. We next answer in what conditions the oscillating combustions could occur in this model of the Mg–O_2 combustion system. It is readily obtained from Fig. 5 or Table 1 that the conditions are $t_0 >$ one constant (47.5) and $t_1 \geq t_0$. Keep in mind that $t_0 = k_2 X_0^b / k_O$ and $t_1 = k_2 X_0^b / k_M$. Therefore, the conditions obtained indicate that k_O must be less than one value and that k_M must be comparable to or less than k_O if oscillations are expected to occur in this Mg–O_2 system. This result can be easily understood. As we know, the magnitude of k_O mainly affects the rate of offering O_2 to the surface of Mg(s) in processes 1 and 2. If k_O is very large, the partial pressure of O_2 existing close to the

Table 1. Nonlinear dynamic behavior of the model in the three regions

Region	Range	Nonlinear dynamic behavior
Region I	$47.5 > t_0 > 0$	Sequentially showing monostability, bistability, and monostability as t_1 increases
Critical case	$t_0 = 47.5$	Just showing monostability with a big leap
Region II	$82.6 > t_0 > 47.5$	Showing two Hopf bifurcation points. Sequentially experiencing a monostable state, a coexisting state for a stable point and a limit cycle, an oscillating state, and a monostable state as t_1 increases. The values of t_1/t_0 at C_1 essentially equal unity
Critical case	$t_0 = 82.6$	One of the two Hopf bifurcation points extends towards the infinite
Region III	$t_0 > 82.6$	Only a monostable state and an oscillating state exist. Compared with region II, the values of t_1/t_0 at C_1 are larger than unity and increase with the increment of t_0

surface of Mg(s) will almost equal that of O_2 in the environment, becoming a constant; consequently, no oscillation can occur. On the other hand, if k_M is markedly greater than k_O, Mg(g) cannot be accumulated, also no oscillation can occur. It should be noted that this result is obtained only from the viewpoint of chemical reaction dynamics, not from the properties of atoms and molecules.

Assume that in this Mg–O_2 combustion system the vapor of Mg diffuses in the form of monoatoms and that Mg gas atoms and O_2 molecules are ideal gases of statistical mechanics, then the crude value of t_1/t_0 can be estimated to be 1.22 (atomic weight of Mg/molecular weight of O_2)$^{1/2}$, which is larger than unity. According to the second condition stated earlier, oscillations could occur in the real system, explaining in part the occurrence of the oscillations observed in the corresponding experiment [17].

On the basis of the linear stability analysis of the simple reaction–diffusion model of the Mg–O_2 solid-phase combustion system, we believe that the diffusion coefficients of reacting gases indeed mightily affect the dynamic behavior of the system. We also obtained some interesting results and phenomena. It would be interesting if these results and phenomena could be examined in real systems.

Acknowledgements. The authors gratefully thank Hong Li Wang for fruitful discussions. This work was supported financially by the National Natural Science Foundations of China (29873006).

References

1. Field RJ, Burger M (1985) Oscillations and traveling waves in chemical systems. Wiley, New York
2. Gray P, Scott SK (1990) Chemical oscillations and instabilities. Non-linear chemical kinetics. Clarendon, Oxford
3. Scott SK (1991) Chemical chaos. Clarendon, Oxford
4. Uppal A, Ray WH, Poore AB (1974) Chem Eng Sci 29:967
5. Uppal A, Ray WH, Poore AB (1976) Chem Eng Sci 31:205
6. Kubicek M, Hofmann H, Hlavacek V, Sinkule J (1980) Chem Eng Sci 35:987
7. Baulch DL, Griffiths JF, Pappin AJ, Sykes AF (1988) Combust Flame 73:163
8. Johnson BR, Griffiths JF, Scott SK (1991) J Chem Soc Faraday Trans 87:523
9. Johnson BR, Griffiths JF, Scott SK, Tomlin AS (1991) J Chem Soc Faraday Trans 87:2539
10. Gray P, Griffiths JF, Scott SK (1984) Proc R Soc Lond Ser A 394:243
11. Scott SK, Wang J, Showalter K (1997) J Chem Soc Faraday Trans 93:1733
12. Pearlman H (1997) J Chem Soc Faraday Trans 93:2487
13. Gol'binder AI, Goryachev VV (1961) Russ J Phys Chem 35:889
14. Merihanov AG, Filonenko AK, Borovinskaya IP (1973) Sov Phys Dokl 208:122
15. Matkowsky BJ, Sivashinsky GI (1978) SIAM J Appl Math 33:465
16. Bayliss A, Matkowshy BJ (1990) SIAM J Appl Math 50:437
17. Feng C-G, Zeng Q-X, Wang L-Q, Fang X (1996) J Chem Soc Faraday Trans 92:2971
18. Liu B-Z (1994) Fundamentals of nonlinear dynamics and chaos (in Chinese). Northeast Normal University Press, Chang Chun
19. Parker TS, Chua LO (1989) Practical numerical algorithms for chaotic systems. Springer, Berlin Heidelberg New York